Journal of Visualization, Vol. 1, No. 3 (1999) 283-290

Flow Visualization for an Unconventional Forebody

Yang, Q. D.*[1], Ma, M. S.*[1], Yu, T.*[1], Hu, H. D.*[1], Zhou, N. C.*[1] and Zhang, J. X.*[2]

*[1] China Aerodynamics Research and Development Center, P.O.Box 211, Mianyang Sichuan, China.
*[2] Harbin Aerodynamics Research Institute, P. O. Box 88, Harbin, China.

Received 20 July 1998.
Revised 20 October 1998.

***Abstract*:** Some results of flow visualization are described for an unconventional fuselage with Erickson-like forebody. The experiment includes force measurement, surface oil flow visualization, and laser sheet flow visualization. Some results are also obtained from a CFD code for solving laminar Navier-Stokes equations. Although there are some differences between the model in the experiment and the model in the computation, the location of vortex on the models exhibits good agreements. The investigation in this paper shows that varying the forebody shape of fuselage can change the flow characteristics greatly and the Erickson-like forebody has potential to improve the lateral-direction stability of the aircraft at high angles of attack.

***Keywords*:** flow visualization, unconventional forebody, high angle of attack.

1. Introduction

As we know, the slender bodies of revolution, especially those having pointed noses, generate asymmetric vortices, side forces and yawing moments at high angles of attack. The general forebodies of fuselage provide directional instability from low to moderate angles of attack, and the vertical tail, which locates in the separated flow region of the fuselage and wing, will lose its control ability at high angles of attack. Therefore, the directional stability of aircraft with this kind of forebodies decreases with increasing of the angle of attack. In order to improve stability of aircraft at high angle of attack, there has been an increasing interest with the noncircular aircraft nose recently[1-7], and the Erickson configuration is one of them. The separate vortices generated from the sharp edges of these configurations are stable and fixed, and do not generate asymmetry side forces at high angles of attack. On the other hand, this kind of noncircular nose can produce asymmetric vortices in sideslip. In this situation in sideslip, the windward vortex is nearer to the surface and induces more suction force than the leeward vortex. This is the reason why these configurations can keep directional stability at high angles of attack.

The investigation in this paper is a part of advanced aircraft configuration research. The major goal of this investigation is to help developing technologies that can significantly improve the performance of aircraft at the high angle of attack. Improving performance of high angles of attack depends on understanding and controlling of the flow. To achieve this, some pictures of flow visualization using laser sheets, surfaces oil flow and numerical results are presented in this paper.

2. Model

The model for the computation is an Erickson-like body. The description of the Erickson model is presented in reference [3]. A portion of a tangent ogive with 19.5° half-apical angle, which is followed by three cubic spline segments, defines the upper surface centerline of the model. A portion of a tangent ogive with 15° half-apical angle

followed by two cubic spline segments and two straight sections define the bottom centerline. A portion of a tangent-ogive with 27.5° half-apical angle defines the maximum half breadth line. The sketch of model for the computation is shown in Fig.1. The experimental model is an aircraft fuselage with the Erickson forebody, but there is only a little difference from the real Erickson configuration at the rear of fuselage.

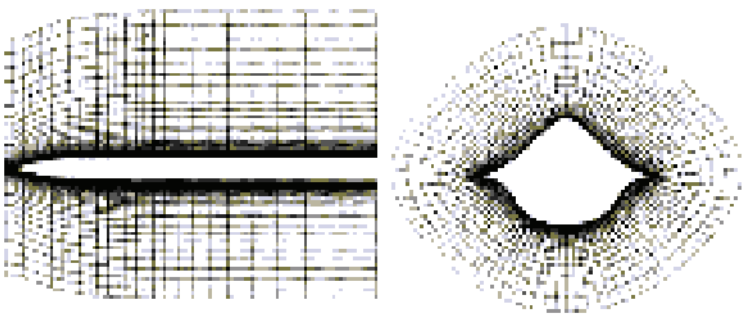

Fig. 1. Sketch of model for the computation.

3. Computational Method

The flow over the Erickson-like forebody is computed using an NS code for solving the Navier-Stokes equations. The Navier-Stokes equations are solved by an implicit difference scheme and LU approximate factor decomposition and maximum eigenvalue split. A well known numerical flux function, Jameson flux function, is used for the inviscid terms, and the center different scheme is used in the viscous terms. The computational grid is generated by algebraic method and smoothed by solving hyperbolic equations. In this case, $47\times40\times89$ cells are used. Figure 1 shows the computational grid. When viscous effects are included, the no-slip and non-penetration boundary condition are enforced on the body surface, and the inflow and outflow boundary conditions are used at far field inflow, outflow and outer boundary respectively. The adiabatic wall condition is assumed.

The calculation Re number is about 4.4×10^5 based on the maximum breadth . The computations are made on the PC 586/166. The computation data correspond to the angles of attack from 12° to 50°, and the angles of sideslip from 0° to 20°. The detail of the method for numerical simulation is referred to the reference [8].

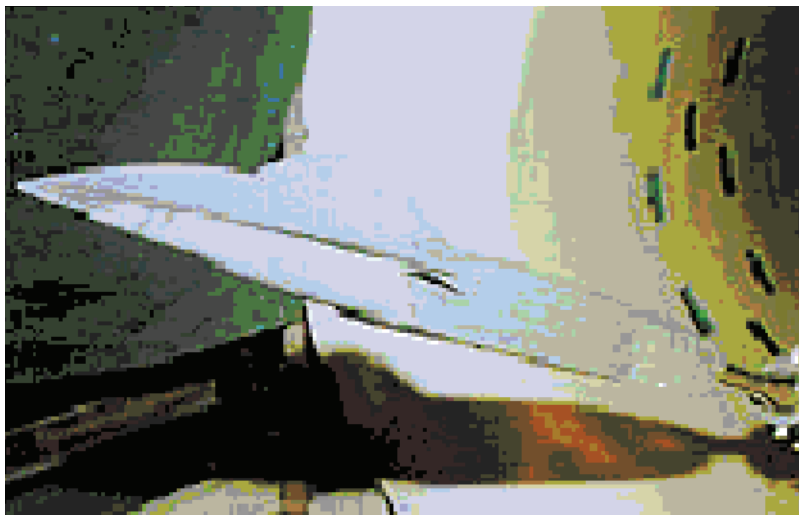

Fig. 2. Model in the test section.

4. Wind Tunnel and Experimental Method

Experiments are conducted in the FL-5 wind tunnel in HARBIN Aerodynamics Research Institute. FL-5 is a low speed return-flow wind tunnel with an open test section. The diameter of the nozzle exit is 1.5m. The range of velocity in the test section varies from 15m/s to 45m/s. The model is mounted in test section by a tail sting supported on the floor. It is capable of providing an angle of attack ranging from 0° to 70° and an angle of sideslip ranging from 0° to 20°.

A six-component internal strain gage balance is used to measure all forces and moments.

An oil flow method is used to visualize the surface flow structure. In this method, a black paint coat is painted on the model surface for the flow field distinctiveness. The mixture of titanium dioxide and kerosene, which is used for surface flow visualization, is painted uniformly on the model surface before testing and photographing.

A laser sheet is used to obtain smoke flow visualization that can determine the movement and location of vortices. In this experiment, a 4- watt argon-ionized laser is placed outside the test section and its output is connected to an optical fiber. A light sheet is generated when the laser beam goes through cylindrical lens at the head of the optical fiber. A low power convergent lens, which is used to compensate the beam natural divergence, is placed downstream of the cylindrical lens to assure the light sheet within the observed field.

In order to get successive illumination of different flow slice at given stations on the model, the head of the optical fiber is placed on an apparatus above the test section which is moveable along a longitudinal axis. The head of optical fiber is also moveable in the rotation direction around the incident beam axis which makes it possible to adjust the light sheet perpendicular to the longitudinal axis of the model in sideslip.

The smoke is used as tracer particles in this test. It is generated by the glycol at temperature above 250℃ and injected into flow field through an emission pipe. The locations of the pipe can be adjusted in order to get a detail observation of the flow field of interest especially those contain vortices.

Cameras and video recorders, which can be placed either outside the test section or within the flow field behind the model, are used to record the images of vortices.

5. Results and Discussion

a. To demonstrate the validity of the CFD code for this study, the computational pressure distribution on the upper surface is compared with that in reference [3]. The comparison in Fig. 3 shows in good agreements except for a lightly difference in the location of the *Cp*min. Based on this comparison, we conclude that the CFD methods can be used to study the flow fields in our investigation.

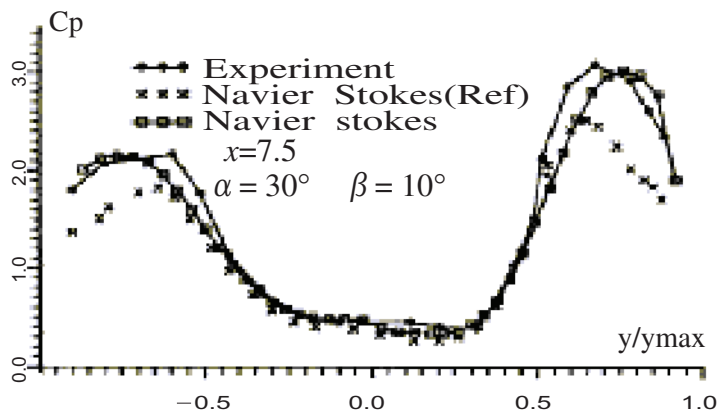

Fig. 3. Comparison of surface distribution.

b. The upper surface pressure distributions of various cross sections on the body at α=30°, β =0° are shown in Fig. 4. It shows that the pressure distribution on the upper surface is symmetric and the peak of suction decreases with the distance increasing from the forebody apex.

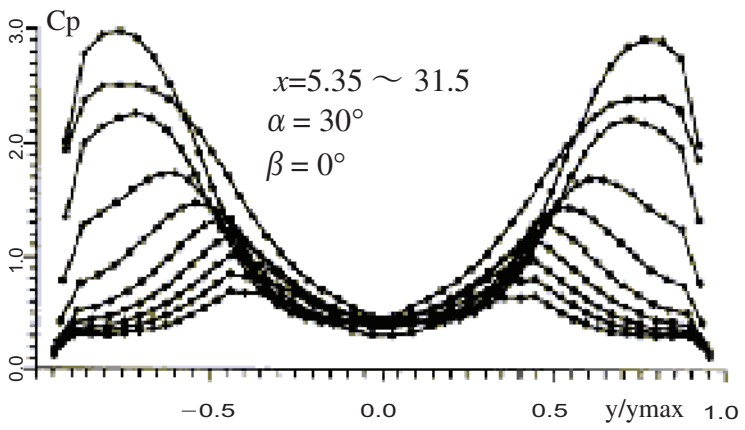

Fig. 4. Upper surface pressure of various stations.

c. The upper surface pressure distributions of various cross sections at α=30°, β=10° are shown in Fig. 5. It shows that the pressure distribution on the upper surface is asymmetric because of the angle of sideslip. The suction peaks of the windward side at β=10° are higher obviously than that at β=0° and the suction peaks of the leeward side are lower obviously than that at β=0°. The suction peaks of the windward are greatly higher than that at leeward. Such great difference of pressure acting on the surface of the forebody results in a stable directional stability.

Fig. 5 also shows that the magnitude of suction peaks decrease with the distance increasing from the forebody apex. However, after the x=22.5, the tendency is inverse. The suction peaks begin to increase with the distance increasing. The reason perhaps is that the vortex of windward sides moves near to the protuberance of the upper surface.

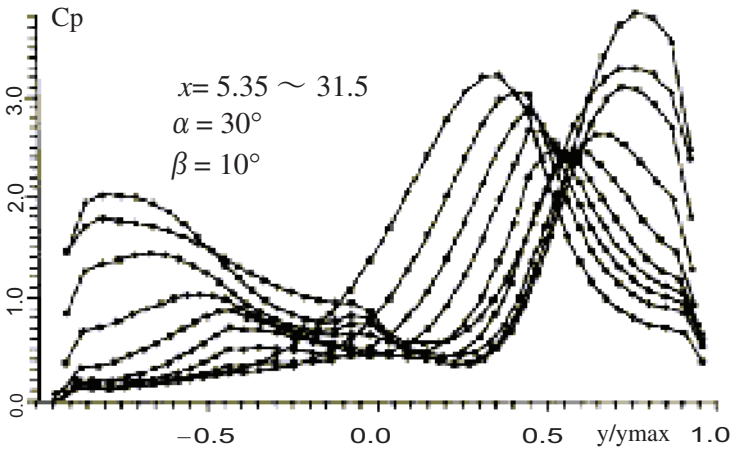

Fig. 5. Upper surface pressure of various stations.

d. The cross sectional streamlines on the various stations obtained by the computation are shown in Fig. 6 at α=30° and β=0°. These figures illustrate that the flow is separated from the sharp edge of the cross section at high angles of attack, and a pair of symmetrical vortices is formed on the upper surface. The vortices cores are enlarged with the distance increasing from the nose of body. The locations of vortices above the upper surface are gradually getting higher, which result in decreasing of induced suction peaks of vortices.

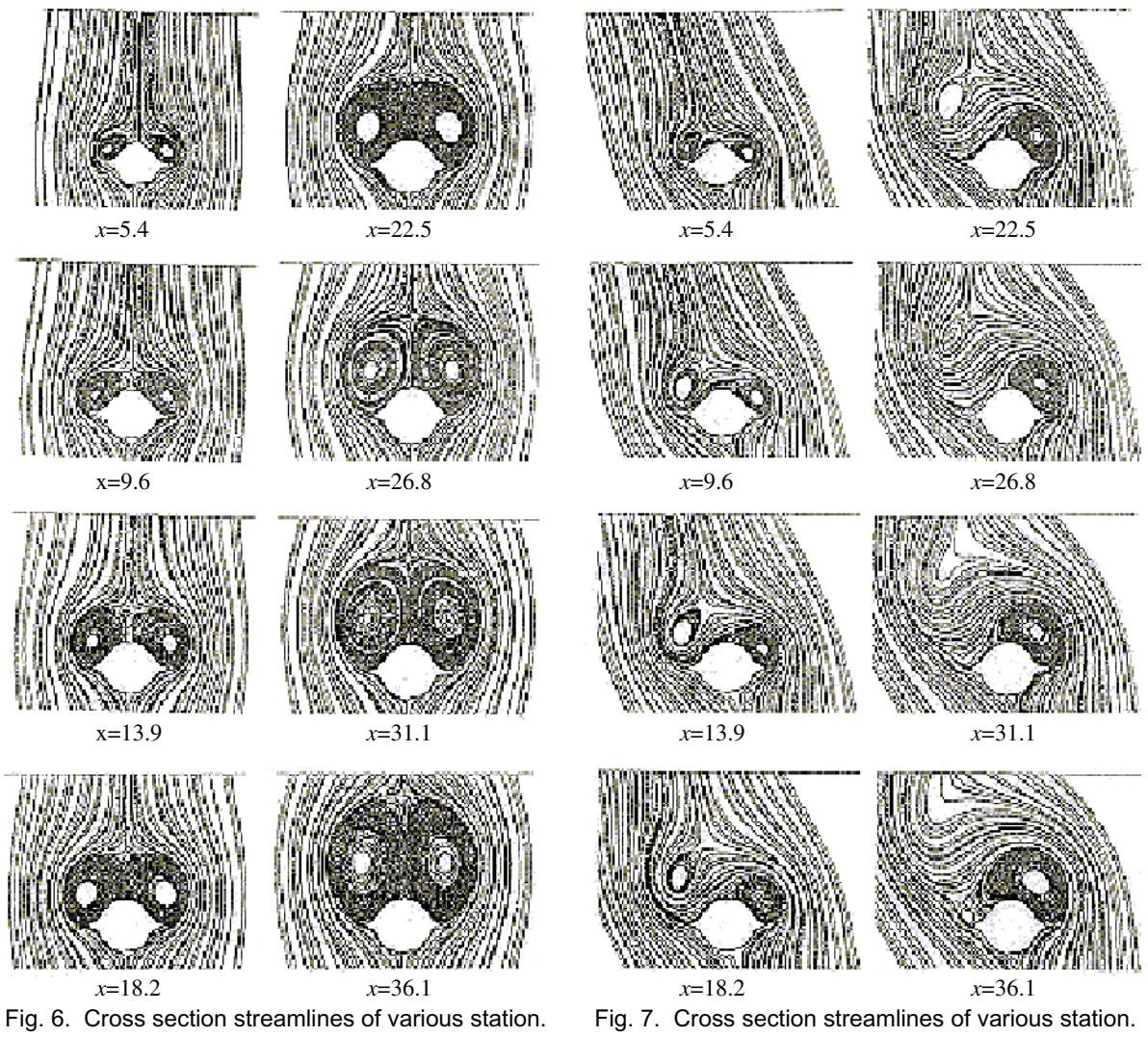

Fig. 6. Cross section streamlines of various station.

Fig. 7. Cross section streamlines of various station.

The cross section streamlines at α=30° and β=10° on various stations are shown in Fig. 7. The locations of upper surface vortices at the windward side are nearer the surface than that at the leeward. It indicates that the asymmetry of separated vortices on the upper surface depends on the combination of angles of attack and sideslip.

e. Laser sheet flow visualization photos at α=30° and β=0°, 5°, 10° on the x=5.4, 14, 18.2 are shown respectively in Fig. 8. At β=0°, a pair of symmetry separated vortices above the upper surface can be seen distinctly. Whenβ=5°, 10°, the vortex at windward side moves toward the surface and the centerline of the upper surface. Meanwhile, the vortex at leeward moves away from the surface. These results are consistent with the results of computation.

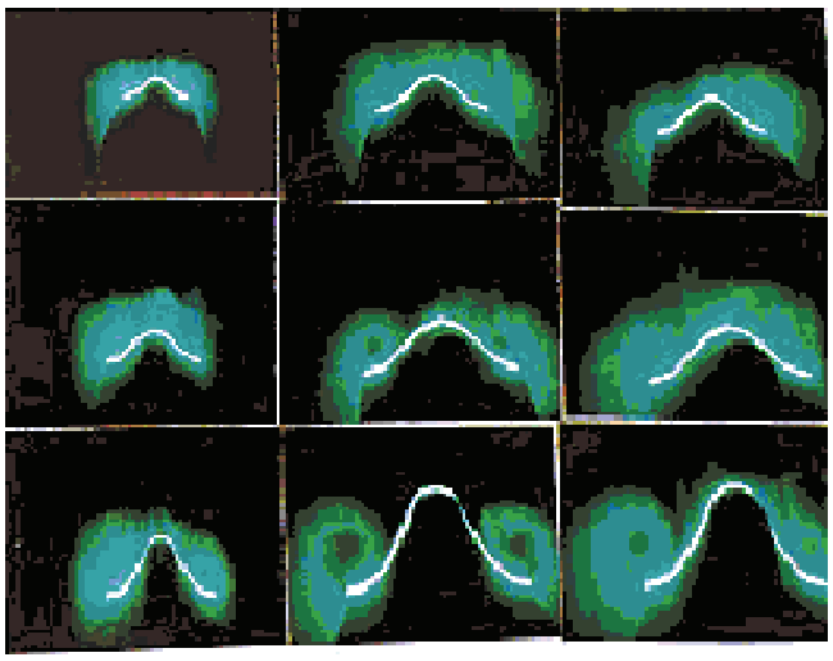

Fig. 8. Laser sheet flow visualization α =12°.

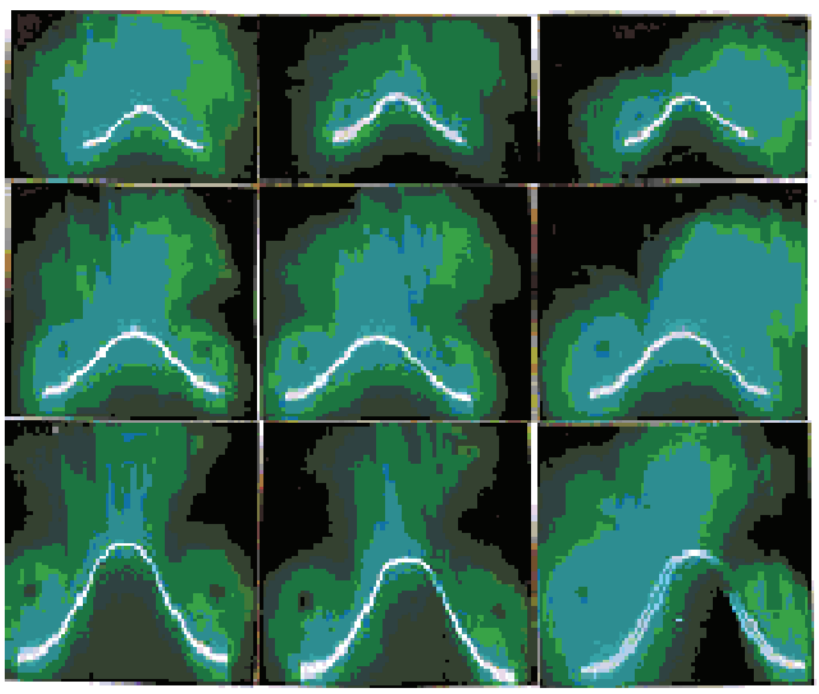

Fig. 8. (continue) α =30°.

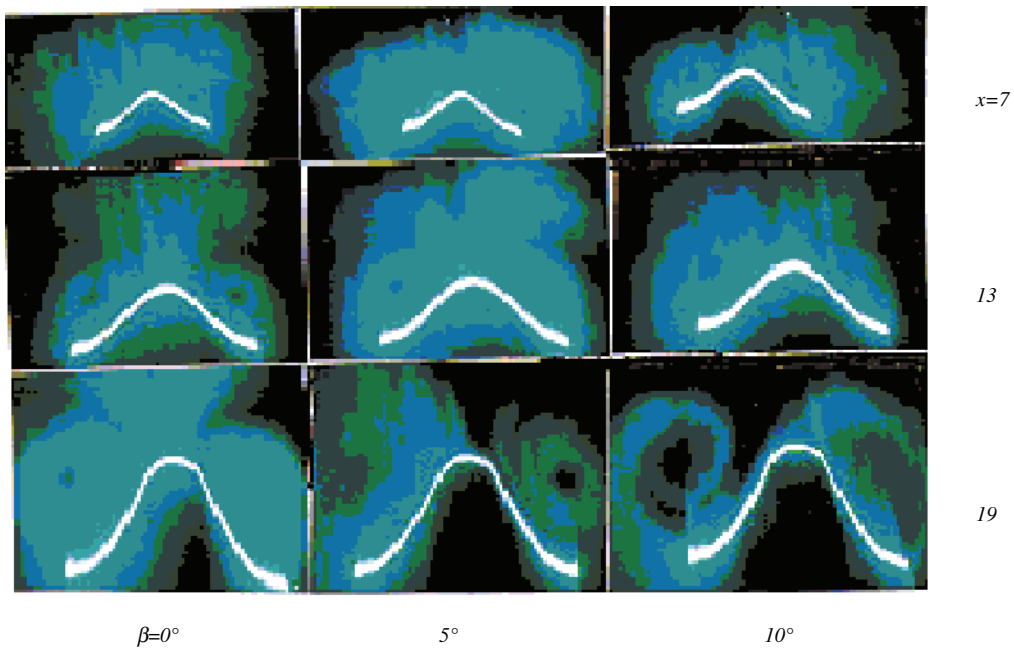

Fig. 8. Laser sheet flow visualization α =12°.

Figure 9 is a photo of vortex traces, which is taken on the side of the wind tunnel with a high luminous auxiliary illumination. Two "black lines" seem to be vortex traces of windward side vortex and leeward side vortex respectively. The trace of the leeward side vortex is higher above the body surface than the windward side one.

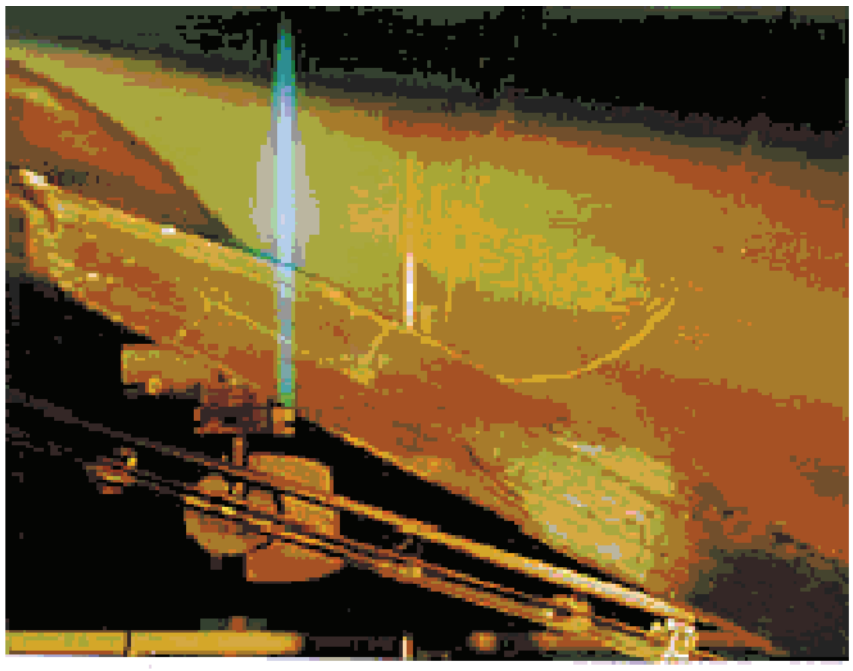

Fig. 9. Photo of vortex traces.

f. The oil flow pictures are shown in Fig. 10 at the α=12°, β=0° and β=5°. The separation lines and attachment lines on the upper surface are very clear on the pictures. From these two pictures, we can find that the separation lines and attachment lines move toward the direction of stream at β=5°. The pictures also show the effects of cockpit.

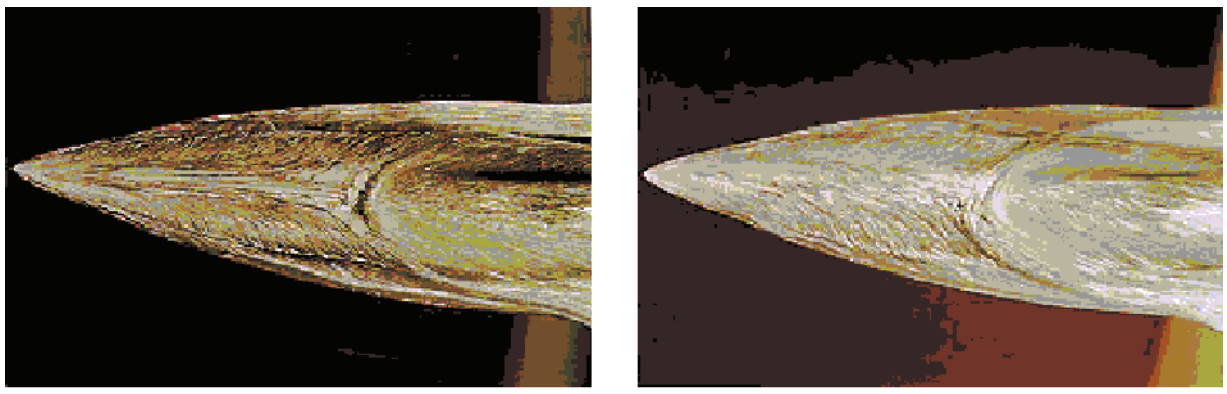

$\beta = 0°$ $\beta = 5°$

Fig. 10. Oil flow pictures α =12°.

6. Conclusions

— The flow fields are dominated by the separated vortices flow at high angles of attack, and a good understanding of this will enable us to design the fighter aircraft with better performance at high angles of attack.

— The Erickson-like forebody has a significant positive contribution to directional stability at angles-of-attack above which the vertical tail ceases to be effective.

— The flow visualization is useful for understanding the flow structure at high angles of attack. CFD methods prove to be valid through the comparison of experimental and other computational results, and we can use these methods to investigate the flow structure.

Acknowledgments

The experimental investigation would not have been possible without the help from the low speed wind tunnel laboratory of HARI. The authors gratefully acknowledge to the contributions of Mr. Huang Changyou.

References

Roos, F. W. and Kegelman, J. T., Aerodynamic Characteristics of Three Generic Forebodies at High Angles of Attack", AIAA Paper 91-275, Jan 1991.

Ravi, R. and Mason, W. H., A Computational Study on Directional Stability of Chine-Shaped Forebodies at High-α", AIAA Paper 92-30, Jan 1992.

Mason, W. H. and Ravi, R., Hi-Alpha Forebody Design: part I Methodology Base and Initial Parametric, VPI-Aero-176(rev.), Jan 1992.

Ravi, R. and Marson, W., Hi-Alpha Forebody Design: Part II Determination of Body shapes for positive Directional stability, VPI-Aero-182(rev.), Feb 1992.

Erickson, G. E. and Brandon, J. M., Low-Speed Experimental Study of the Vortex Flow Effects of a Fighter Forebody Having Unconventional Cross Section, AIAA Paper 85-1798, Aug 1985.

Erickson, G. E., On the Non-Linear Aerodynamics and Stability Characteristics of a Generic Chine-Forebody Slender-Wing Fighter Configuration, AIAA Paper 87-2617, Aug 1987.

Yang, Q. D. Ma, M.S., et al., A Primary Research for An Unconventional Forebody, CARDC EJ-9-94011, Jun 1994.

Yu, T., Numerical Simulation of Complex configuration, CARDC EJ report, Aug 1995.

Authors' Profiles

Yang Qide: He received his bachelor's in the Department of aircraft in 1961 from Beijing Aeronautical and Astronautical University. Now, he works as a research professor in the Computational Aerodynamics Institute of China Aerodynamics Research and Development Center. He is also the visiting professor of Beijing Aeronautical and Astronautical University and Nanjing Aeronautical and Astronautical University. He interests in applied aerodynamics including layout of aircraft and computational methods.